Field-induced ferromagnetic exchange interaction in metamagnetic transitions of heavy-electron liquids

Hiroyuki Satoh and Fusayoshi J. Ohkawa
Department of Physics, Hokkaido University, Sapporo 060, Japan
(Received 26 June 1997)

The metamagnetic transition or crossover in $CeRu_2Si_2$ is investigated using the Hubbard model, with a pseudogap structure of the density of states of quasiparticles phenomenologically taken into account. Local quantum spin fluctuations are considered through mapping to the Anderson model. Intersite effects are considered by the $1/d$ expansion method, with d being the spatial dimensionality. There are two main driving forces in the metamagnetic transition: a field-dependent exchange interaction and the magnetostriction or the Kondo volume-collapse effect. The exchange interaction due to the virtual exchange of pair excitations within the quasiparticle band changes its signs with increasing magnetization. It is antiferromagnetic in the absence of fields and is ferromagnetic in the vicinity of the metamagnetic point. The pseudogap structure plays a critical role in this sign change. This exchange interaction scales with the bandwidth of the quasiparticles, and the single-parameter scaling approximately holds for the magnetization and the magnetostriction processes. [S0163-1829(98)10009-7]

I. INTRODUCTION

$CeRu_2Si_2$ is a heavy-electron compound with a large electronic specific-heat coefficient of $\gamma \simeq 350$ mJ/mol K^2.[1] One of the main features of this compound is a sharp increase of magnetization around an external field of $H_M \simeq 7.7$ T, when the field is applied along the c axis of the tetragonal structure.[2] Although it seems to be a crossover,[3] it is conventionally called a metamagnetic transition. Not only the magnetization process but also many other physical properties are anomalous in this field region of $H_M \cong 7.7$ T. For example, the magnetostriction is large and the molar volume V exhibits an abrupt increase around H_M.[4,5] On the other hand, this compound has a large Grüneisen constant of $\Gamma \equiv -\partial \ln T_K / \partial \ln V \simeq 190$.[6] Here, T_K is the local Kondo temperature and is an energy scale of local quantum spin fluctuations. The combination of the large magnetostriction and the large Grüneisen constant leads to the conclusion that T_K decreases significantly with increasing magnetization.

Various theoretical investigations have been performed to explain the metamagnetic transition. Miyake and Kuramoto[7] have calculated the magnetization process using a semiphenomenological model called the duality model. Konno[8] has argued that the crystal-field splitting plays a critical role. Evans[9] has argued that the anisotropy of the hybridization matrix plays a critical role. All of these mechanisms are purely electronic.

On the other hand, metamagnetic transitions of the first order have been observed in other transition-metal alloys rather than f-electron systems. Yamada[10,11] has investigated the metamagnetic transitions in transition-metal alloys. Two effects are important according to his arguments: a ferromagnetic exchange interaction and a pseudogap structure around the chemical potential. It is quite easy to see that when these two effects are large enough a metamagnetic transition easily occurs.

It is certain that the competition between the quenching of magnetic moments by the local quantum spin fluctuations and a ferromagnetic exchange interaction is a key issue to understand the magnetic transition of heavy-electron systems. The decrease of T_K makes the development of magnetization easy. This magnetostriction effect should also be taken into account to explain the metamagnetic transition of $CeRu_2Si_2$. One of the authors of this paper has investigated the metamagnetic transition by taking into account this magnetostriction effect[12] and a pseudogap structure.[13] However, he assumed a phenomenological ferromagnetic exchange interaction. The observed magnetization process of $CeRu_2Si_2$ obeys the single-parameter scaling.[4] This scaling imposes a strong restriction on a relevant ferromagnetic exchange interaction responsible for the metamagnetic transition.

The $1/d$ expansion method has been developed in a previous paper,[14] with d being the spatial dimensionality. One of the greatest advantages of this method is that the local quantum spin fluctuations can be properly taken into account in the single-site approximation (SSA).[14] Then, the $1/d$ expansion method is physically *a perturbative method of treating intersite effects, starting from the SSA*. Various physical properties of strongly correlated electron systems have already been investigated by the $1/d$ expansion method: high-temperature superconductivity in the vicinity of the Mott transition,[14] the crossover between sinusoidal and helical magnetic structures,[15] magnetic exchange interactions in alloys,[16] and the mode-mode coupling effect between spin fluctuations.[17] The purpose of this paper is to investigate the metamagnetic transition of heavy-electron liquids by the $1/d$ expansion method.

II. FORMULATION

A. Model

One of the simplest effective Hamiltonians for heavy-electron liquids is the periodic Anderson model. A gap or a

pseudogap structure of the density of states is inherent in this model because of the hybridization between an almost dispersionless f band and conduction bands. This pseudogap structure can be taken into account even within the Hubbard model when a phenomenological density of states is used. Then, we start with the Hubbard model in d dimensions:

$$\mathcal{H}_H=\sum_{ij\sigma} t_{ij}f_{i\sigma}^{\dagger}f_{j\sigma}+\frac{1}{2}U\sum_{i\sigma} f_{i\sigma}^{\dagger}f_{i\sigma}f_{i-\sigma}^{\dagger}f_{i-\sigma}. \quad (2.1)$$

Here, $f_{i\sigma}^{\dagger}$ and $f_{i\sigma}$ are creation and annihilation operators of f electrons with spin σ at site $\mathbf{R}_i$, respectively. The transfer integrals t_{ij} include dimensional factors to retain the model nontrivial in the large-d limit; for example, $t_{ij}=O(1/\sqrt{d})$ for nearest neighbors.[18] The density of states of unrenormalized electrons is given by

$$\rho_0(\varepsilon)=\frac{1}{N}\sum_{\mathbf{k}} \delta(\varepsilon-E(\mathbf{k})), \quad (2.2)$$

with N being the number of unit cells and $E(\mathbf{k})=\Sigma_j t_{ij}e^{-i\mathbf{k}\cdot(\mathbf{R}_i-\mathbf{R}_j)}$. In this paper, it is assumed that $\rho_0(\varepsilon)$ has a camel-back structure around $\varepsilon\simeq\varepsilon_f$, with $\varepsilon_f\equiv t_{ii}$ being a band center. It is also assumed for the sake of simplicity that the system is symmetrical so that $\rho_0(\varepsilon_f+\varepsilon)=\rho_0(\varepsilon_f-\varepsilon)$ and $\varepsilon_f-\mu=-U/2$, with μ being the chemical potential. It follows that $\Sigma_\sigma\langle f_{i\sigma}^{\dagger}f_{i\sigma}\rangle_H=1$, where $\langle\cdots\rangle_H$ means the statistical average for the Hamiltonian (2.1). We will confine our study to $T=0$ K and the large-d limit ($d\to+\infty$).

The single-particle Green function is written as

$$G_\sigma(i\varepsilon_n,\mathbf{k})=\frac{1}{i\varepsilon_n+\mu-E(\mathbf{k})-\tilde{\Sigma}_\sigma(i\varepsilon_n)} \quad (2.3)$$

in the wave-number representation. Here, $\tilde{\Sigma}_\sigma(i\varepsilon_n)$ is the irreducible single-site self-energy function. The multisite self-energy vanishes in the large-d limit. The Green function in the site representation is written as $R_{ij\sigma}(i\varepsilon_n)=(1/N)\Sigma_{\mathbf{k}}e^{i\mathbf{k}\cdot(\mathbf{R}_i-\mathbf{R}_j)}G_\sigma(i\varepsilon_n,\mathbf{k})$. Calculating the single-site self-energy is reduced to solving a mapped Anderson model (MAM):

$$\mathcal{H}_A=\sum_{\mathbf{k}\sigma} \varepsilon_c(\mathbf{k})c_{\mathbf{k}\sigma}^{\dagger}c_{\mathbf{k}\sigma}+\sum_{\sigma} \varepsilon_f f_\sigma^{\dagger}f_\sigma + \frac{1}{\sqrt{N}}\sum_{\mathbf{k}\sigma}[V(\mathbf{k})c_{\mathbf{k}\sigma}^{\dagger}f_\sigma+V^*(\mathbf{k})f_\sigma^{\dagger}c_{\mathbf{k}\sigma}] + \frac{1}{2}U\sum_{\sigma} f_\sigma^{\dagger}f_\sigma f_{-\sigma}^{\dagger}f_{-\sigma}. \quad (2.4)$$

The three quantities of μ, ε_f, and U for the MAM Eq. (2.4) are the same as those for the Hubbard model (2.1), respectively. The combination of $\varepsilon_c(\mathbf{k})$ and $V(\mathbf{k})$ is determined through the mapping condition of $R_{ii\sigma}(i\varepsilon_n)=\tilde{G}_\sigma(i\varepsilon_n)$, where

$$\tilde{G}_\sigma(i\varepsilon_n)=\frac{1}{i\varepsilon_n+\mu-\varepsilon_f-\tilde{\Sigma}_\sigma(i\varepsilon_n)-L(i\varepsilon_n)} \quad (2.5)$$

is the Green function for the MAM, with

$$L(i\varepsilon_n)=\frac{1}{\pi}\int_{-\infty}^{\infty}d\varepsilon\,\frac{\Delta(\varepsilon)}{i\varepsilon_n-\varepsilon} \quad (2.6)$$

and

$$\Delta(\varepsilon)=\frac{\pi}{N}\sum_{\mathbf{k}}|V(\mathbf{k})|^2\delta(\varepsilon+\mu-\varepsilon_c(\mathbf{k})). \quad (2.7)$$

Because the Hubbard model is symmetrical, it follows that $\Delta(\varepsilon)=\Delta(-\varepsilon)$.

The self-energy of the MAM is expanded so that $\tilde{\Sigma}_\sigma(i\varepsilon_n)=\tilde{\Sigma}_0+[1-\tilde{\phi}_m]i\varepsilon_n+\cdots$. The dispersion relation of quasiparticles is given by $\xi(\mathbf{k})=[E(\mathbf{k})-\varepsilon_f]/\tilde{\phi}_m$, where the relation of $\mu-\varepsilon_f-\tilde{\Sigma}_0=0$ for the symmetrical model has been used. The density of states of the quasiparticles is given by

$$\rho^*(\varepsilon)=\frac{1}{N}\sum_{\mathbf{k}} \delta(\varepsilon-\xi(\mathbf{k}))=\tilde{\phi}_m\rho_0(\tilde{\phi}_m\varepsilon+\varepsilon_f). \quad (2.8)$$

The coherent part of Eq. (2.3) is written as

$$G_\sigma^{(c)}(i\varepsilon_n,\mathbf{k})=\frac{1}{\tilde{\phi}_m}\frac{1}{i\varepsilon_n-\xi(\mathbf{k})}. \quad (2.9)$$

The corresponding coherent part of Eq. (2.5) is given by

$$\tilde{G}_\sigma^{(c)}(i\varepsilon_n)=\frac{1}{\tilde{\phi}_m i\varepsilon_n-L^{(c)}(i\varepsilon_n)}, \quad (2.10)$$

with

$$L^{(c)}(i\varepsilon_n)=\tilde{\phi}_m i\varepsilon_n-\left[\frac{1}{\tilde{\phi}_m}\int_{-\infty}^{\infty}d\xi\,\frac{\rho^*(\xi)}{i\varepsilon_n-\xi}\right]^{-1}. \quad (2.11)$$

B. Electron-lattice interaction

The local Kondo temperature T_K is defined by

$$[\tilde{\chi}_s(+i0)]_{T=0\ \mathrm{K}}\equiv 1/k_BT_K, \quad (2.12)$$

where $\tilde{\chi}_s(i\omega_l)$ is the spin susceptibility of the MAM.[14] In the large-U region, there exists another small parameter, $s_K\equiv k_BT_K/U$, in addition to $1/d$. Because $s_K\simeq 10^{-4}$ in $CeRu_2Si_2$, only leading-order or zeroth-order terms in s_K are considered in this paper.

The volume dependence of T_K is approximately written as[12]

$$T_K(x)=T_K(0)e^{-x} \quad (2.13)$$

with

$$x=\Gamma(v-v_0)/v_0, \quad (2.14)$$

where v and v_0 are volumes of a unit cell in the presence and the absence of magnetic fields and pressures, respectively. In this paper, the magnetostriction effect is taken into account only through the volume dependence of T_K. As is discussed in the Appendix, $\tilde{\phi}_m$ is inversely proportional to T_K. Then, it follows that

$$\tilde{\phi}_m(x)=\tilde{\phi}_m(0)e^{x}, \quad (2.15)$$

$$\rho^*(\varepsilon;x)=\rho^*(\varepsilon e^x;0)e^x, \tag{2.16}$$

and

$$L^{(c)}(i\varepsilon_n;x)=L^{(c)}(i\varepsilon_n e^x;0). \tag{2.17}$$

C. Thermodynamic potential

In order to calculate magnetization m and the molar volume or x in the presence of magnetic fields H and pressures P, it is convenient to consider the thermodynamic potential given by

$$\Omega=\Omega_0+\Omega_f+mH^*+P^*x \tag{2.18}$$

per unit cell, where Ω_0 is the thermodynamic potential for the lattice system, $P^*=(v_0/\Gamma)P$ and $H^*=g\mu_B H/2$, with g being an effective g factor and μ_B being the Bohr magneton. The second term is given by

$$\Omega_f=-\frac{1}{N\beta}\ln(\mathrm{Tr}[e^{-\beta(\mathcal{H}'-\mu\mathcal{N})}]), \tag{2.19}$$

where $\beta=1/k_BT$, $\mathcal{N}=\Sigma_{i\sigma}f^\dagger_{i\sigma}f_{i\sigma}$, and

$$\mathcal{H}'=\mathcal{H}_H+\mathcal{H}_Z \tag{2.20}$$

with

$$\mathcal{H}_Z=\frac{1}{4}NU(m^2-p^2)-\sum_{i\sigma}\left(\frac{1}{2}Um+H^*-\frac{1}{2}Up\right)\sigma f^\dagger_{i\sigma}f_{i\sigma} \tag{2.21}$$

is a fictitious Hamiltonian. It should be noted that when m is equal to p, $\mathcal{H}_Z$ becomes the conventional Zeeman term and $\mathcal{H}'$ is reduced to the Hubbard model (2.1) with the Zeeman energy. As will be shown below, a treatment of this thermodynamic potential gives $m=p$.

Ferromagnetic moments along the z direction are calculated as a function of m, p, H^*, and x so that $p'=\Sigma_\sigma\sigma\langle f^\dagger_{i\sigma}f_{i\sigma}\rangle$. Here, $\langle\cdots\rangle$ means the statistical average for the Hamiltonian $\mathcal{H}'$. We require that

$$p'=p. \tag{2.22}$$

Because p' is a function of m, p, H^*, and x, this equation defines p as a function of m, H^*, and x. Then, it is easy to see that

$$\left(\frac{\partial\Omega}{\partial p}\right)_{m,H^*,x}=-\frac{1}{2}U(p-p')=0 \tag{2.23}$$

and

$$\left(\frac{\partial\Omega}{\partial m}\right)_{H^*,x}=\frac{1}{2}U(m-p')+H^*. \tag{2.24}$$

Hence the condition of

$$\left(\frac{\partial\Omega}{\partial m}\right)_{H^*,x}=H^* \tag{2.25}$$

is equivalent to $m=p=\Sigma_\sigma\sigma\langle f^\dagger_{i\sigma}f_{i\sigma}\rangle$. Eventually m and x are determined by Eq. (2.25) and

$$\left(\frac{\partial\Omega}{\partial x}\right)_{m,H^*}=0. \tag{2.26}$$

The thermodynamic potential Ω is calculated perturbatively in terms of p and $\bar{m}\equiv m+2H^*/U$ from $\mathcal{H}_Z$ in addition to the many-body interaction of U. Instead of Ω itself, we consider $(\partial\Omega/\partial m)_{H^*,x}$ because the summation of diagrams becomes easy. The Hartree terms are divided into two terms so that

$$U\langle f^\dagger_{i-\sigma}f_{i-\sigma}\rangle=U\langle f^\dagger_{i-\sigma}f_{i-\sigma}\rangle_H-\frac{1}{2}\sigma Up'. \tag{2.27}$$

Here, the first term is the Hartree term for the Hamiltonian (2.1) and is called the normal Hartree term; the second term is called the anomalous Hartree term. Fully renormalized anomalous Hartree terms are canceled by corresponding p terms from $\mathcal{H}_Z$ because of the requirement (2.22). Then, the procedure of calculating $(\partial\Omega/\partial m)_{H^*,x}$ is as follows: First, sum up all skeleton diagrams. Here, the skeleton diagrams consist of the single external point $\partial/\partial m$, anomalous $\bar{m}$ terms from $\mathcal{H}_Z$, many-body U lines from $\mathcal{H}_H$, and unperturbed Green functions, but any part which belongs to the anomalous Hartree term should be excluded. The skeleton diagrams are divided into single-site and multisite diagrams. When only the same site indices appear in diagrams in the site representation, they are the single-site diagrams. All the other diagrams are the multisite diagrams. Second replace the unperturbed Green functions by the renormalized ones, $R_{ij\sigma}$'s.

The thermodynamic potential is described as follows:

$$\Omega(m,x;H^*,P)=\Omega_{\mathrm{para}}(x)+\tilde{\Omega}(\bar{m},x)+\Delta\Omega(\bar{m},x)-(H^*)^2/U+P^*x. \tag{2.28}$$

Here, the first term is the thermodynamic potential for the paramagnetic state given by $\Omega_{\mathrm{para}}(x)=\Omega_0(x)+\Omega_f(m=0,H^*=0,x)$. Because the compressibility of $CeRu_2Si_2$ remains almost constant when pressures change,[19] we assume that

$$\Omega_{\mathrm{para}}(x)=\Omega_{\mathrm{para}}(0)+k_BT_K(0)\frac{1}{2\kappa}x^2, \tag{2.29}$$

where κ is a dimensionless compressibility. The second and third terms of Eq. (2.28) are the magnetic single-site and the magnetic multisite terms, respectively. The magnetic single-site term $\tilde{\Omega}(\bar{m},x)$ is defined so that it includes $U\bar{m}^2/4=Um^2/4+mH^*+(H^*)^2/U$. Because of this definition, $(H^*)^2/U$ has been subtracted in Eq. (2.28). For strongly correlated systems, however, $(H^*)^2/U$ can be ignored.

The magnetic single-site part is calculated from the following Hamiltonian:

$$\tilde{\mathcal{H}}'=\mathcal{H}_A+\tilde{\mathcal{H}}_Z, \tag{2.30}$$

with

$$\widetilde{\mathcal{H}}_Z=\frac{1}{4}U(m^2-\widetilde{p}^{\,2})-\sum_\sigma\left(\frac{1}{2}Um+H^*-\frac{1}{2}U\widetilde{p}\right)\sigma f_\sigma^\dagger f_\sigma, \tag{2.31}$$

where m and H^* are the same as those of Eq. (2.21), and $\widetilde{p}$ is given by $\widetilde{p}=\Sigma_\sigma\sigma\langle f_\sigma^\dagger f_\sigma\rangle_A$, with $\langle\cdots\rangle_A$ standing for the statistical average for the Hamiltonian (2.30). There is an exact one-to-one correspondence between the perturbative series for the derivative of thermodynamic potential with respect to m for the Hamiltonian (2.30) and that for $(\partial\widetilde{\Omega}/\partial m)_{H^*,x}$.

Although the MAM should be determined through the mapping condition, we approximately use results for the Anderson model with an infinitely large U and a constant hybridization energy $\Delta(\varepsilon)=\Delta$, which are obtained in the Appendix. It is easy to see that

$$\left(\frac{\partial\widetilde{\Omega}}{\partial m}\right)_{H^*,x}=\frac{1}{2}Um+H^*-\frac{1}{2}U\widetilde{p}. \tag{2.32}$$

Then, it follows that

$$\left(\frac{\partial\widetilde{\Omega}}{\partial m}\right)_{H^*,x}=k_BT_K(x)\,\frac{m}{\sqrt{1-m^2}} \tag{2.33}$$

to leading order in s_K, where Eq. (A5) has been made use of.

The irreducible self-energy and the three-point vertex functions for the Hamiltonian (2.30), denoted by $\widetilde{\Sigma}_\sigma^{(A)}(i\varepsilon_n;\overline{m},x)$, and $\widetilde{\lambda}_{\sigma\sigma'}^{(A)}(i\varepsilon_n,i\varepsilon_n+i\omega_l;\overline{m},x)$, respectively, are related with each other through the Ward-Takahashi identity[20] so that

$$\frac{\partial}{\partial m}\widetilde{\Sigma}_\sigma^{(A)}(i\varepsilon_n;\overline{m},x)=-\frac{1}{2}U\sum_{\sigma'}\sigma'\widetilde{\lambda}_{\sigma'\sigma}^{(A)}(i\varepsilon_n,i\varepsilon_n;\overline{m},x). \tag{2.34}$$

A magnetic part of the self-energy given by

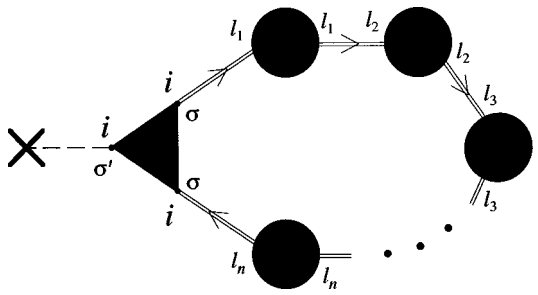

FIG. 1. Diagram for $(\partial\Delta\Omega/\partial m)_{H^*,x}$. A cross stands for $\partial/\partial m$, a double line with an arrow for the Green function $R_{ij\sigma}$, a dotted line for U from $\mathcal{H}_Z$, a large circle for the self-energy part $\delta\widetilde{\Sigma}_\sigma^{(A)}$ and a triangle for the vertex part $\widetilde{\lambda}_{\sigma'\sigma}^{(A)}$. The local portion of $l_1=l_2=\cdots=l_n=i$ should be excluded.

$$\delta\widetilde{\Sigma}_\sigma^{(A)}(i\varepsilon_n;\overline{m},x)=\widetilde{\Sigma}_\sigma^{(A)}(i\varepsilon_n;\overline{m},x)-\widetilde{\Sigma}_\sigma^{(A)}(i\varepsilon_n;0,x) \tag{2.35}$$

is expanded according to the Appendix so that

$$\delta\widetilde{\Sigma}_\sigma^{(A)}(i\varepsilon_n;\overline{m},x)=\delta\widetilde{\Sigma}_\sigma^{(A)}(0;\overline{m})-\widetilde{\phi}_m(x)[r(m)-1]i\varepsilon_n+\cdots \tag{2.36}$$

with

$$\delta\widetilde{\Sigma}_\sigma^{(A)}(0;\overline{m})=-\sigma\Delta\,\tan\left(\frac{\pi}{2}m\right) \tag{2.37}$$

and

$$r(m)=\frac{(1-m^2)^{3/2}}{\cos^2((\pi/2)m)} \tag{2.38}$$

to leading order in s_K.

For the magnetic multisite part, we consider the diagram shown in Fig. 1. It gives

$$\left(\frac{\partial\Delta\Omega}{\partial m}\right)_{H^*,x}=\frac{1}{\beta}\sum_{\varepsilon_n\sigma}\left(\frac{\partial}{\partial m}\delta\widetilde{\Sigma}_\sigma^{(A)}(i\varepsilon_n;\overline{m},x)\right)_{H^*,x}\times\left\{\frac{1}{N}\sum_{\mathbf{k}}\frac{1}{[G_\sigma(i\varepsilon_n,\mathbf{k};x)]^{-1}-\delta\widetilde{\Sigma}_\sigma^{(A)}(i\varepsilon_n;\overline{m},x)}-\frac{1}{[\widetilde{G}_\sigma(i\varepsilon_n;x)]^{-1}-\delta\widetilde{\Sigma}_\sigma^{(A)}(i\varepsilon_n;\overline{m},x)}\right\}. \tag{2.39}$$

Here, the local term has been subtracted. When Eqs. (2.33) and (2.39) are integrated, the thermodynamic potential is obtained so that

$$\Omega=k_BT_K(x)(1-\sqrt{1-m^2})+k_BT_K(0)\frac{1}{2\kappa}(x-x_0)^2-\frac{1}{\beta}\sum_{\varepsilon_n\sigma}\left\{\frac{1}{N}\sum_{\mathbf{k}}\ln(1-G_\sigma(i\varepsilon_n,\mathbf{k};x)\delta\widetilde{\Sigma}_\sigma^{(A)}(i\varepsilon_n;m,x))-\ln(1-\widetilde{G}_\sigma(i\varepsilon_n;x)\delta\widetilde{\Sigma}_\sigma^{(A)}(i\varepsilon_n;m,x))\right\}+C, \tag{2.40}$$

to leading order in s_K, with $x_0=-\kappa P^*/k_BT_K(0)$ being an equilibrium value of x in the presence of pressures P at zero field, and $C=\Omega_{\text{para}}(0)-k_BT_K(0)x_0^2/2\kappa$.

D. Magnetic exchange interactions

Equation (2.25) becomes

$$H^*=k_BT_K(x)\frac{m}{\sqrt{1-m^2}}-\frac{1}{4}\int_0^m J(m',x)dm', \tag{2.41}$$

where $J(m,x)$ is defined by

$$\frac{1}{4}\int_0^m J(m',x)dm' = -\left(\frac{\partial \Delta\Omega}{\partial m}\right)_{H^*,x} \tag{2.42}$$

or

$$\frac{1}{4}J(m,x) = -\left(\frac{\partial^2 \Delta\Omega}{\partial m^2}\right)_{H^*,x}. \tag{2.43}$$

Because Eq. (2.41) gives

$$\lim_{H^*\to 0}\left(\frac{\partial m}{\partial H^*}\right)_x = \frac{1}{k_B T_K(x) - J(0,x)/4}, \tag{2.44}$$

$J(0,x)$ defined by Eqs. (2.42) or (2.43) is nothing but the intersite exchange interaction of the Hubbard model.[14]

The right side of Eq. (2.42) is given by Eq. (2.39). The summation over ε_n in Eq. (2.39) can be divided into two parts: that over $|\varepsilon_n| \gg k_B T_K(0)$ and that over $|\varepsilon_n| \lesssim 2k_B T_K(0)$. According to this division, $J(m,x)$ is also divided into two parts:

$$J(m,x) = J_s + J_Q(m,x). \tag{2.45}$$

The first term J_s is the high-energy contribution. It is calculated from Eq. (2.43) in the same approximation as that used in a previous paper[21] so that $J_s = -\Sigma_j 4t_{ij}^2/U$. It is nothing but the superexchange interaction within the Hubbard model. In an extended model, however, whether it is ferromagnetic or antiferromagnetic depends on the whole band structure.[16] In this paper, therefore, we treat J_s as a phenomenological exchange interaction. It is obvious that it scarcely depends on m and x.

The second term, $J_Q(m,x)$, is the low-energy contribution within the quasiparticle band. It follows from Eqs. (2.9), (2.10), and (2.36) that

$$\frac{1}{4}\int_0^m J_Q(m',x)dm' = \sum_\sigma \int_{-\infty}^0 d\varepsilon \left(\frac{\partial E_\sigma(\varepsilon,m,x)}{\partial m}\right) \times \{F(E_\sigma(\varepsilon,m,x),E_\sigma(\varepsilon,m,x);x) - F(E_\sigma(\varepsilon,m,x),\varepsilon;x)\}, \tag{2.46}$$

with

$$F(\varepsilon_1,\varepsilon_2;x) = \left(-\frac{1}{\pi}\,\mathrm{Im}\right)\frac{1}{\varepsilon_1 - L^{(c)}(\varepsilon_2+i0;x)/\tilde{\phi}_m(x)}, \tag{2.47}$$

and

$$E_\sigma(\varepsilon,m,x) = r(m)\varepsilon + \sigma\frac{4k_B T_K(x)}{\pi}\tan\left(\frac{\pi}{2}m\right), \tag{2.48}$$

to leading order in s_K. It should be noted that $F(\varepsilon,\varepsilon;x) = \rho^*(\varepsilon;x)$. When Eqs. (2.15), (2.16), and (2.17) are used, it is easy to see that $J_Q(m,x) = e^{-x}J_Q(m,0)$ and $J_Q(m,x)$ scales with T_K. Then, it is described as

$$J_Q(m,x) \equiv k_B T_K(x)\,\overline{J_Q}(m), \tag{2.49}$$

where $\overline{J_Q}(m)$ does not have any explict x dependence. Equation (2.26) becomes

$$0 = k_B T_K(x)\left\{-(1-\sqrt{1-m^2}) + \frac{1}{\kappa}(x-x_0)e^x + \frac{1}{4}\int_0^m dm' \int_0^{m'} dm''\,\overline{J_Q}(m'')\right\}. \tag{2.50}$$

When m and x are calculated as functions of H^* from Eqs. (2.41) and (2.50), the specific-heat coefficient is given by

$$\gamma(H^*) = \frac{1}{3}\pi^2 k_B^2 \frac{1}{N}\sum_{\mathbf{k}\sigma}\left(-\frac{1}{\pi}\,\mathrm{Im}\right) \times \tilde{\phi}_m(x) r(m)\,\frac{1}{[G_\sigma(+i0,\mathbf{k};x)]^{-1} - \delta\tilde{\Sigma}_\sigma^{(A)}(0;m,x)} = \frac{1}{3}\pi^2 k_B^2 r(m)\sum_\sigma \rho^*(E_\sigma(0,m,x);x) \tag{2.51}$$

according to the Fermi-liquid relation.[22]

III. APPLICATION

For the phenomenological exchange interaction from the virtual exchange of high-energy spin excitations, it is assumed that $J_s/[4k_B T_K(0)] = 0.17$ and this value of J_s does not depend on m and x. It is also assumed that the Wilson ratio for the MAM to be two. Then, the density of states at the Fermi level is written as

$$\rho^*(0;x) = 1/4k_B T_K(x) \tag{3.1}$$

from Eq. (A11). The specific-heat coefficient at zero field is given by $\gamma(0) = \pi^2 k_B^2/[6k_B T_K(0)]$ from Eqs. (2.51) and (3.1). From the observed value of $\gamma(0) \simeq 350$ mJ/mol K^2, T_K is evaluated so that $T_K(0) = 39$ K for $CeRu_2Si_2$.[23] From the observed compressibility of about[6] 0.95(Mbar)$^{-1}$ together with $T_K(0) = 39$ K, $\Gamma \simeq 190$ and $v_0 = 86.28$ Å^3,[24] the dimensionless compressibility is evaluated so that $\kappa = 2.1$. However, we use $\kappa = 2.2$ to fit a calculated magnetostriction curve on experimental data.

In order to reproduce the camel back structure of the density of states of the quasiparticles, we use the following phenomenological model:

$$\rho^*(\varepsilon;x) = \frac{1}{k_B T_K(x)}\left\{\frac{c_1}{2}[D(\bar{\varepsilon};c_2,c_3) + D(\bar{\varepsilon};-c_2,c_3)] + (1-c_1)D(\bar{\varepsilon};0,c_4)\right\}, \tag{3.2}$$

with $\bar{\varepsilon} = \varepsilon/k_B T_K(x)$, and

$$D(x;a,b) = \frac{1}{\pi}\frac{b}{(x-a)^2+b^2}. \tag{3.3}$$

In Eq. (3.2), c_1, c_2, c_3, and c_4 are dimensionless parameters. Because there exists a restriction of Eq. (3.1), all of c_1, c_2, c_3, and c_4 are not independent of each other. Among

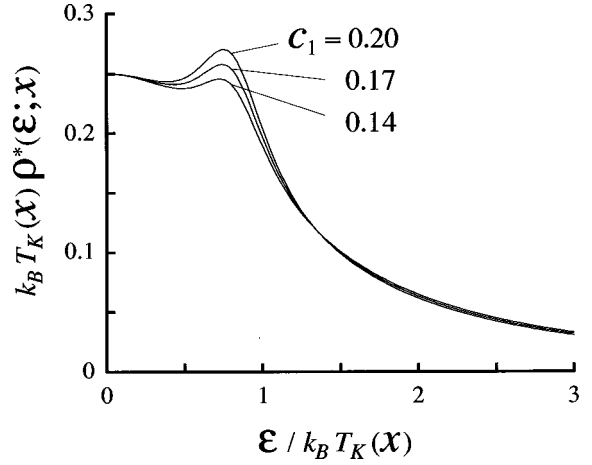

FIG. 2. Density of states $\rho^*(\varepsilon;x)$ multiplied by $k_B T_K(x)$ for various c_1.

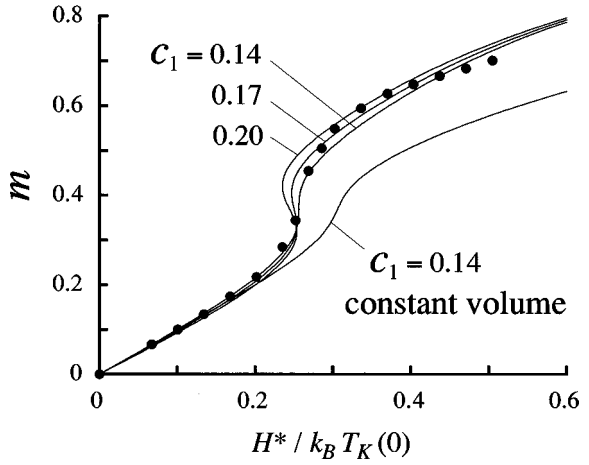

FIG. 4. Magnetization m as a function of $H^*/k_B T_K(0)$. Experimental data[2] are shown by dots.

them, $c_2 = 0.80$ and $c_3 = 0.28$ are assumed in this paper; only c_1 is treated as a variable parameter.

Figure 2 shows $\rho^*(\varepsilon;x)$ for three cases of c_1: $c_1 = 0.14$, 0.17, and 0.20. Figure 3 shows $\bar{J}_Q(m)$ for the three cases of c_1. This exchange interaction is not rigid when m changes; it is antiferromagnetic for small m, while it becomes ferromagnetic around the metamagnetic transition region. When m increases, the density of states goes upward and downward for each spin component with a slight change of the bandwidth occurring. When the peaks in the density of states lie around the chemical potential, the exchange interaction J_Q reaches its maximum value. This tendency is quite physical; when there is a sharp peak around the chemical potential in a broad spectrum, in general, ferromagnetic instability occurs rather than antiferromagnetic instability.

Figures 4 and 5 show the magnetization and the magnetostriction curves in the absence of pressures for each values of c_1. Experimental data[2,5] are also plotted in Figs. 4 and 5, with the saturated magnetization being assumed to be $1.95\mu_B$. Figure 4 also shows the constant volume magnetization process calculated for $c_1 = 0.14$. It has been confirmed that the lattice expansion effect certainly enhances the metamagnetic transition.

Figure 6 shows the specific-heat coefficients $\gamma(H^*)/\gamma(0)$ given by Eq. (2.51) with observed data.[25] The enhancement of $\gamma(H^*)$ in the transition region agrees with the observed enhancement.

In the presence of pressures, it is convenient to rewrite T_K as $T_K(x) = T_K(x_0)e^{-(x-x_0)}$ in Eqs. (2.41) and (2.49). Figure 7 shows the magnetization curves for $c_1 = 0.14$ and for $P = 0$, 1 kbar, and 2 kbars. The values of $T_K(x_0)/T_K(0)$ are 1.20 and 1.43 for $P = 1$ kbar and 2 kbars, respectively. The single-parameter scaling approximately holds for the magnetization process. Because $(x-x_0)e^x \simeq (x-x_0)e^{x_0}$ for $|x-x_0| \ll 1$, it follows from Eq. (2.50) that $(x-x_0)e^{x_0}$ is also approximately scaled in such a way that

$$(x-x_0)e^{x_0} = \psi(H^* e^{x_0}). \tag{3.4}$$

This scaling relation has already been obtained by using thermodynamic relations.[26] Figure 8, which shows the magnetostriction curves for $c_1 = 0.14$ and for $P = 0$, 1 kbar, and 2 kbars, confirms the single-parameter scaling.

The dimensionless compressibility is given by

$$\kappa(H^*) = \kappa \lim_{P \to 0} \left(\frac{\partial x}{\partial x_0} \right)_{H^*} \tag{3.5}$$

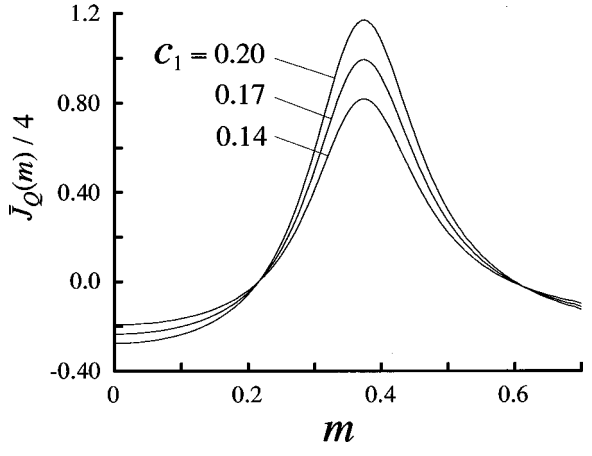

FIG. 3. Exchange interaction $\bar{J}_Q(m)$ multiplied by 1/4.

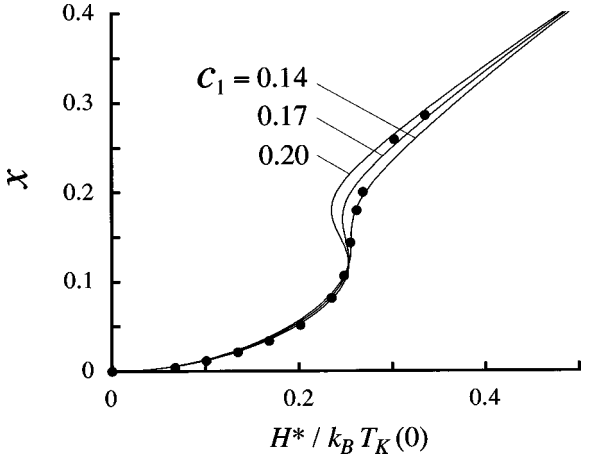

FIG. 5. Magnetostriction $x = \Gamma(v - v_0)/v_0$ as a function of $H^*/k_B T_K(0)$. Experimental data[5] are shown by dots.

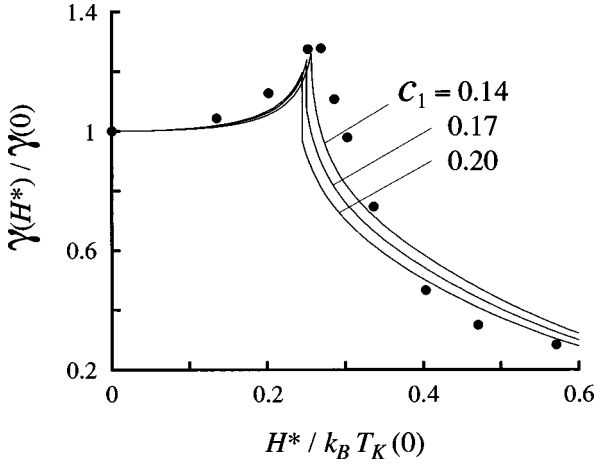

FIG. 6. Specific-heat coefficient as a function of $H^*/k_B T_K(0)$. Experimental data (Ref. 25) are shown by dots.

in the presence of fields. It follows from the scaling relation that

$$\kappa(H^*)/\kappa = 1 - e^{-x_0}\psi(H^* e^{x_0}) + H^*\psi'(H^* e^{x_0}). \quad (3.6)$$

The fact of the derivative of ψ being large in the metamagnetic region shows that the compressibility is enhanced and the lattice becomes soft.

IV. DISCUSSION

The magnetic part of the self-energy for the Hamiltonian (2.20) in the large-d limit, denoted by $\delta\tilde{\Sigma}_\sigma(\varepsilon_n;\overline{m})$, is divided into single-site and multisite terms according to the definition in Sec. II so that

$$\delta\tilde{\Sigma}_\sigma(i\varepsilon_n;\overline{m}) = \delta\tilde{\Sigma}_\sigma^{(A)}(i\varepsilon_n;\overline{m}) + \delta\tilde{\Sigma}'_\sigma(i\varepsilon_n;\overline{m}), \quad (4.1)$$

with $\delta\tilde{\Sigma}'_\sigma(i\varepsilon_n;\overline{m})$ being the multisite term. Here, we have omitted the parameter x. Figure 9 shows an example of the multisite diagrams that do not vanish even in the large-d limit. In Eq. (2.39), a part of the effects of $\delta\tilde{\Sigma}'_\sigma(i\varepsilon_n;\overline{m})$ is included because the vertex correction is included. In Eq. (2.51), no effects of $\delta\tilde{\Sigma}'_\sigma(i\varepsilon_n;\overline{m})$ are included. According to the Fermi-liquid relation, the derivative susceptibility of the Hubbard model is given by

$$\chi_s = \sum_\sigma \left[-\frac{\partial\delta\tilde{\Sigma}_\sigma(i\varepsilon_n;\overline{m})}{\partial H^*} \right]_{H^*\to 0} \rho_0(\varepsilon_f) \quad (4.2)$$

for $m=0$. When the polarization of conduction electrons is taken into account, the derivative susceptibility of the MAM is also given by Eq. (4.2). On the other hand, when the polarization of conduction electrons is not taken into account, the derivative susceptibility is given by

$$\tilde{\chi}_s = \sum_\sigma \left[-\frac{\partial\delta\tilde{\Sigma}_\sigma^{(A)}(i\varepsilon_n;\overline{m})}{\partial H^*} \right]_{H^*\to 0} \rho_0(\varepsilon_f). \quad (4.3)$$

It is reasonable to assume that a similar relation holds for nonzero m. This consideration implies that there is another small parameter in this formulation, the ratio of the polarization of conduction electrons to that of f electrons in the MAM. It has been assumed in this paper that this ratio is small enough and Anderson's compensation theorem[27] approximately holds for the MAM.

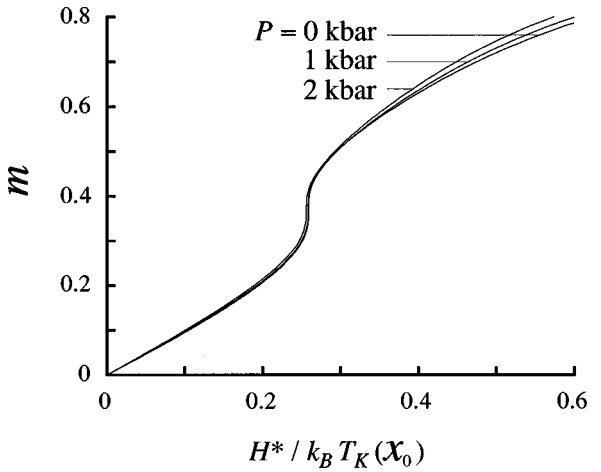

FIG. 7. Magnetization m as a function of $H^*/k_B T_K(x_0)$ for various pressures.

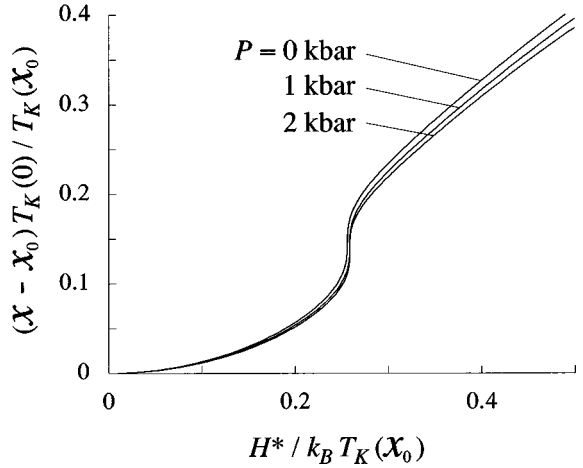

FIG. 8. Magnetostriction $x - x_0$ multiplied by $T_K(0)/T_K(x_0)$ as a function of $H^*/k_B T_K(x_0)$ for various pressures.

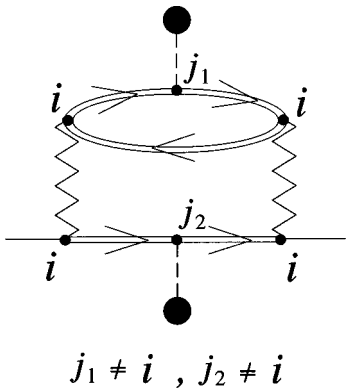

FIG. 9. Example of the multisite diagrams that do not vanish even in the large-d limit. A wavy line stands for U from $\mathcal{H}_H$, and a small circle for the one-body potential $U\overline{m}/2$ from $\mathcal{H}_Z$.

The field dependence of the exchange interaction J_Q is consistent with the observation by neutron-scattering experiments[28] that the antiferromagnetic correlations observed at zero field are suppressed in the metamagnetic transition region. The collapse of the antiferromagnetic correlations is not a driving force of the metamagnetic transition.

A distribution of T_K, which is suggested by the positive magnetoresistance at low field,[29] has not been considered in this paper. If we take into account this effect, the molar magnetization curve will be blurred.

The results of this paper are consistent with the observed data for the magnetization process and the magnetostriction curves. However, because the theoretical results substantially depend on parameters included in the model, it is desirable to use a more practical model such as obtained from band calculations. It is also desirable to solve the MAM self-consistently.

Our investigation has so far been restricted to the metamagnetic transitions in heavy-electron liquids. According to Yamada's calculation,[10] a pseudogap structure exists in transition-metal alloys that exhibit metamagnetic transitions. It is interesting to reexamine metamagnetic transitions in other transition-metal alloys within the theoretical framework of this paper. In particular, it is interesting to examine whether or not the sign change of the exchange interaction is responsible for the transitions.

V. SUMMARY

The metamagnetic transition in $CeRu_2Si_2$ has been studied using the single-band Hubbard model by the $1/d$ expansion method. The local quantum spin fluctuations have been taken into account through mapping to the Anderson model. Effects of intersite magnetic exchange interaction have been taken into account to leading order in $1/d$. All the higher-order effects in $1/d$ have been ignored such as the mode-mode coupling between intersite spin fluctuations.

The exchange interaction mediated by the virtual exchange of spin excitations within the quasiparticle band reflects the camel back structure of the density of states, and it changes its signs and magnitudes with the variation of magnetization. It is definitely ferromagnetic around the metamagnetic transition point. Because its magnitude scales with the bandwidth of the quasiparticles, the magnetization and the magnetostriction processes approximately obey the single-parameter scaling. The sign change and the scaling of the exchange interaction as well as the magnetostriction effect are crucial in the mechanism for the metamagnetic transition proposed in this paper.

ACKNOWLEDGMENTS

The authors are thankful to Toshiro Sakakibara, Takafumi Kita, and Kazuyuki Matsuhira for useful discussions and comments. This work was partly supported by a Grant-in-Aid for Scientific Research (C) No. 08640434 from the Ministry of Education, Science, Sports, and Culture of Japan.

APPENDIX: ANDERSON MODEL IN THE LARGE-U LIMIT

In this appendix, it is assumed that $U/\Delta(0)\to+\infty$ and $\Delta(\varepsilon)$ is independent of ε so that $\Delta(\varepsilon)=\Delta$. The ground-state energy of the Hamiltonian (2.30) measured from the Fermi vacuum energy is approximately written as[30]

$$\widetilde{E}_G=\varepsilon_f-\frac{\Delta}{\pi}\ln\frac{D}{\Delta}-\sqrt{(k_BT_K)^2+(\widetilde{E}_Z)^2}, \tag{A1}$$

with $\widetilde{E}_Z=\frac{1}{2}Um+H^*-\frac{1}{2}U\widetilde{p}$ and

$$k_BT_K=\sqrt{D\Delta}\,\exp\left(\frac{\pi(\varepsilon_f-\mu)}{2\Delta}\right), \tag{A2}$$

with D being a half of the conduction-band width. The volume dependence of T_K is approximately given by Eq. (2.13) with the Grüneisen constant

$$\Gamma=\frac{\pi(\mu-\varepsilon_f)}{2\Delta}\left[v\frac{\partial}{\partial v}\ln\frac{\mu-\varepsilon_f}{\Delta}\right]_{v=v_0}. \tag{A3}$$

When the f level is so deep that $(\mu-\varepsilon_f)/\Delta\gg1$, it is likely that $\Gamma\gg1$.

It follows from Eq. (A1) that

$$\widetilde{p}=\frac{\partial\widetilde{E}_G}{\partial\widetilde{E}_Z}=\frac{\widetilde{E}_Z}{\sqrt{(k_BT_K)^2+(\widetilde{E}_Z)^2}}. \tag{A4}$$

When $|\widetilde{E}_Z|/k_BT_K\ll1$, Eq. (A4) becomes $\widetilde{p}=\widetilde{E}_Z/k_BT_K$. Therefore, the definition of T_K by Eqs. (A1) and (A2) is consistent with the definition by Eq. (2.12). When Eq. (A4) is solved for $\widetilde{p}$, we obtain

$$\widetilde{p}=m+\frac{2H^*}{U}-\frac{2k_BT_K(x)}{U}\frac{m}{\sqrt{1-m^2}}+O(s_K^2). \tag{A5}$$

The self-energy is expanded so that

$$\widetilde{\Sigma}_\sigma^{(A)}(i\varepsilon_n;\overline{m},x)=\widetilde{\Sigma}_\sigma^{(A)}(0;\overline{m},x)+[1-\widetilde{\varphi}_m(\overline{m},x)]i\varepsilon_n\ . \tag{A6}$$

According to the Friedel sum rule,[31] the number of electrons with spin σ is given by

$$\frac{1}{2}(1+\sigma\widetilde{p})=\frac{1}{2}-\frac{1}{\pi}\tan^{-1}\left(\frac{\delta\widetilde{\Sigma}_\sigma^{(A)}(0;\overline{m},x)}{\Delta}\right), \tag{A7}$$

where the relations of $\varepsilon_f-\mu+\widetilde{\Sigma}_0=0$ and $\mathrm{Re}\,L(+i0)=0$ for the symmetrical model have been approximately made use of Eq. (A7) gives

$$\delta\widetilde{\Sigma}_\sigma^{(A)}(0;\overline{m},x)=-\sigma\Delta\,\tan\left(\frac{\pi}{2}\,\widetilde{p}\right). \tag{A8}$$

The derivative of $\widetilde{p}$ with respect to $\widetilde{E}_Z$ can be calculated in the two ways from Eqs. (A4) and (A7). When these two are compared to each other, it follows that

$$\frac{1}{k_BT_K(x)}(1-\widetilde{p}^2)^{3/2}=2\widetilde{\varphi}_s(\overline{m},x)\frac{1}{\pi\Delta}\cos^2\left(\frac{\pi}{2}\,\widetilde{p}\right), \tag{A9}$$

with

$$\tilde{\varphi}_s(\bar{m},x) = -\frac{\partial}{\partial \tilde{E}_Z}\tilde{\Sigma}_\sigma^{(A)}(0;\bar{m},x). \tag{A10}$$

When charge fluctuations are completely suppressed, $\tilde{\varphi}_s(\bar{m},x)/\tilde{\varphi}_m(\bar{m},x)=2$ is satisfied.[32] Then, it follows from Eq. (A9) that

$$\tilde{\varphi}_m(0,x) = \tilde{\phi}_m(x) = \pi\Delta/4k_BT_K(x), \tag{A11}$$

and

$$\frac{\tilde{\varphi}_m(\bar{m},x)}{\tilde{\varphi}_m(0,x)} = \frac{\tilde{\varphi}_s(\bar{m},x)}{\tilde{\varphi}_s(0,x)} = (1-\tilde{p}^2)^{3/2}\Big/\cos^2\left(\frac{\pi}{2}\tilde{p}\right). \tag{A12}$$

It should be noted that $\tilde{p}=\bar{m}=m$ to leading order in s_K.

[1] M. J. Besnus, J. P. Kappler, P. Lehmann, and A. Meyer, Solid State Commun. **55**, 779 (1985).
[2] P. Haen, J. Flouquet, F. Lapierre, P. Lejay, and G. Remenyi, J. Low Temp. Phys. **67**, 391 (1987).
[3] T. Sakakibara, T. Tayama, K. Matsuhira, H. Mitamura, H. Amitsuka, K. Maezawa, and Y. Onuki, Phys. Rev. B **51**, 12 030 (1995).
[4] L. Puech, J. M. Mignot, P. Lejay, P. Haen, J. Flouquet, and J. Voiron, J. Low Temp. Phys. **70**, 237 (1988).
[5] C. Paulsen, A. Lacerda, L. Puech, P. Haen, P. Lejay, J. L. Tholence, J. Flouquet, and A. de Visser, J. Low Temp. Phys. **81**, 317 (1990).
[6] A. Lacerda, A. de Visser, P. Haen, P. Lejay, and J. Flouquet, Phys. Rev. B **40**, 8759 (1989).
[7] K. Miyake and Y. Kuramoto, J. Magn. Magn. Mater. **90&91**, 438 (1990).
[8] R. Konno, J. Phys.: Condens. Matter **3**, 9915 (1991).
[9] S. M. M. Evans, J. Magn. Magn. Mater. **108**, 135 (1992).
[10] H. Yamada, Physica B **149**, 390 (1988).
[11] H. Yamada, Phys. Rev. B **47**, 11 211 (1993).
[12] F. J. Ohkawa, Solid State Commun. **71**, 907 (1989).
[13] F. J. Ohkawa, Prog. Theor. Phys. Suppl. **108**, 209 (1992).
[14] F. J. Ohkawa, Phys. Rev. B **54**, 15 388 (1996).
[15] F. J. Ohkawa, K. Onoue, and H. Satoh, J. Phys. Soc. Jpn. **67**, 535 (1998).
[16] F. J. Ohkawa, J. Phys. Soc. Jpn. **67**, 525 (1998).
[17] F. J. Ohkawa, Phys. Rev. B **57**, 412 (1998).
[18] W. Metzner and D. Vollhardt, Phys. Rev. Lett. **62**, 324 (1989).
[19] P. Haen, J.-M. Laurant, K. Payer, and J.-M. Mignot, in *Transport and Thermal Properties of f-Electron Systems*, edited by G. Oomi *et al.* (Plenum, New York, 1993), p. 145.
[20] J. C. Ward, Phys. Rev. **78**, 182 (1950).
[21] F. J. Ohkawa and N. Matsumoto, J. Phys. Soc. Jpn. **63**, 602 (1994).
[22] J. M. Luttinger, Phys. Rev. **119**, 1153 (1960).
[23] The value of $T_K=39$ K in this paper is $\pi/2$ times as large as $T=24$ K in the previous papers (Refs. 1–3) because of different definitions of T_K, and these two values of T_K are consistent with each other.
[24] K. Hiebl, C. Horvath, P. Rogl, and M. J. Sienko, J. Magn. Magn. Mater. **37**, 287 (1983).
[25] H. P. van der Meulen, A. de Visser, J. J. M. Franse, T. T. J. M. Berendschot, J. A. A. J. Perenboom, H. van Kempen, A. Lacerda, P. Lejay, and J. Flouquet, Phys. Rev. B **44**, 814 (1991).
[26] K. Matsuhira, T. Sakakibara, H. Amitsuka, K. Tenya, K. Kamishima, T. Goto, and G. Kido, J. Phys. Soc. Jpn. **66**, 2851 (1997).
[27] P. W. Anderson, Phys. Rev. **124**, 41 (1961).
[28] J. Rossat-Mignod, L. P. Regnault, J. L. Jacoud, C. Vettier, P. Lejay, J. Flouquet, E. Walker, D. Jaccard, and A. Amato, J. Magn. Magn. Mater. **76&77**, 376 (1988).
[29] F. J. Ohkawa, Phys. Rev. Lett. **64**, 2300 (1990).
[30] T. Yamamoto and F. J. Ohkawa, J. Phys. Soc. Jpn. **57**, 3562 (1988).
[31] H. Shiba, Prog. Theor. Phys. **54**, 967 (1975).
[32] A. Yoshimori, Prog. Theor. Phys. **55**, 67 (1976).